Received: 3 April 2022 | Revised: 1 August 2022 | Accepted: 3 August 2022

DOI: 10.1002/jcc.26994

RESEARCH ARTICLE

Journal of COMPUTATIONAL CHEMISTRY WILEY

Structure and bonding of proximity-enforced main-group dimers stabilized by a rigid naphthyridine diimine ligand

Jonas Weiser[1,2,3] | Jingjing Cui[4] | Rian D. Dewhurst[1,2] | Holger Braunschweig[1,2] | Bernd Engels[3] | Felipe Fantuzzi[1,2,5]

[1]Institute for Inorganic Chemistry, Julius-Maximilians-Universität Würzburg, Würzburg, Germany

[2]Institute for Sustainable Chemistry & Catalysis with Boron, Julius-Maximilians-Universität Würzburg, Würzburg, Germany

[3]Institute for Physical and Theoretical Chemistry, Julius-Maximilians-Universität Würzburg, Würzburg, Germany

[4]School of Chemistry and Environmental Engineering, Wuhan Institute of Technology, Wuhan, People's Republic of China

[5]School of Chemistry and Forensic Science, University of Kent, Canterbury, UK

Correspondence
Felipe Fantuzzi, School of Chemistry and Forensic Science, University of Kent, Park Wood Rd, Canterbury CT2 7NH, UK.
Email: f.fantuzzi@kent.ac.uk

Funding information
Deutsche Forschungsgemeinschaft

Abstract

The development of ligands capable of effectively stabilizing highly reactive main-group species has led to the experimental realization of a variety of systems with fascinating properties. In this work, we computationally investigate the electronic, structural, energetic, and bonding features of proximity-enforced group 13–15 homodimers stabilized by a rigid expanded pincer ligand based on the 1,8-naphthyridine (*napy*) core. We show that the redox-active naphthyridine diimine (NDI) ligand enables a wide variety of structural motifs and element-element interaction modes, the latter ranging from isolated, element-centered lone pairs (e.g., E = Si, Ge) to cases where through-space π bonds (E = Pb), element-element multiple bonds (E = P, As) and biradical ground states (E = N) are observed. Our results hint at the feasibility of NDI-E_2 species as viable synthetic targets, highlighting the versatility and potential applications of *napy*-based ligands in main-group chemistry.

KEYWORDS
bond theory, computational chemistry, density functional calculations, main group elements, N ligands

1 | INTRODUCTION

The last few decades have witnessed significant advances in the synthesis and isolation of persistent molecular compounds featuring highly reactive element–element (E–E) single and multiple bonds. The interest in such systems is very broad, ranging from the investigation of fundamental aspects related to electronic structure and bonding situation of molecules[1] to applications in various fields, such as small-molecule activation[2] and catalysis.[3] The success in the experimental realization of such intriguing main-group systems was made possible through the development of ligands capable of stabilizing highly reactive bonding motifs. Particularly, N-heterocyclic carbenes (NHCs)[4] and related systems, such as cyclic alkyl(amino) carbenes (CAACs),[5] have been successfully employed for this task, and their use in main-group chemistry has paved the way for the discovery of new classes of compounds and bonding arrangements. These include, but are not limited to, diborenes (B═B),[6] diborynes (B≡B),[2c,7] a diborabutatriene (C═B═B═C),[8] an L—Si_2H_2—L compound[9] (L = Lewis base), a diphosphabutadiene (C═P—P═C),[10] tetraphosphatrienes (P═P═P═P),[11] as well as ^{Dip}NHC–PN–CAAC (Dip = diisopropylphenyl), the first experimentally characterized base-stabilized heterodiatomic compound.[12]

Remarkably, these ligands have also been used as molecular platforms for stabilizing compounds with unusual metal–metal bonds,[13] as well as biradicals and biradicaloids,[14] findings that have motivated recent computational investigations.[15] The outstanding performance of NHCs and CAACs in facilitating the synthesis of compounds featuring unusual E—E bonds has stimulated the search for new potential ligands in main-group chemistry. For example, Hermann and Frenking[16] applied density functional theory (DFT) and energy

decomposition analysis with natural orbitals for chemical valence (EDA-NOCV)[17] calculations to investigate the use of carbones (CL_2), which can be portrayed as four-electron, double Lewis-base donors, in the formation of $E[CL_2]_2$ (E = Be, B^+, C^{2+}, N^{3+}, Mg, Al^+, Si^{2+}, P^{3+}) ligands. Saha et al.[18] computationally explored the electronic structure and stability of $B_2(MIC)_2$ complexes (MIC = mesoionic carbene), whose high endergonicity for the dissociation of the B—B and B—L bonds hints at their experimental feasibility. Some of us also examined the potential use of biscarbenes to stabilize oligomers, nanowires, and nanowheels featuring boron–boron triple bonds.[19] Similar investigations have been performed for analyzing hitherto unknown NHC-stabilized main-group heterodimers, such as Si—C,[20] P—Si,[21] and P—Al.[22]

Another important class of systems with applications in the fixation and stabilization of main group elements and dimers is that based on tetradentate ligands. These include tetrapyrrolic macrocycles from the porphyrinoid family, such as porphyrins,[23] phthalocyanines,[24] and corroles,[25] as well as expanded pincer ligands.[26] Some systems of the latter category feature non-rigid, acyclic structures based on for example bis-imide groups, while others contain cyclic, rigid backbones, such as those related to the 1,8 naphthyridine (*napy*) core. Indeed, *napy* derivatives are known to be capable of forming diverse coordination patterns with transition metals and main-group Lewis acids.[27] These systems have been applied in distinct fields, including as fluorescence,[28] two-photon absorption,[29] photoluminescence,[30] and sensing materials.[31] Recently, some of us reported that the diphosphino-functionalized 1,8-naphthyridine (NDP) ligand can be used as a ligand platform for boranes and diboranes.[32] Furthermore, by employing the redox-active, rigid naphthyridine diimine (NDI) ligand (Figure 1A), we were able to isolate a geometry-constrained bis(germylene) species by the reduction of its dichloro precursor.[33]

The NDI ligand has proven to be a very promising platform for supporting bimetallic cooperation. An NDI-Ni_2 complex was found to be able to catalyze [4 + 1] cycloaddition reactions of 1,3-dienes and vinylidenes, thus providing a direct synthetic entry into polysubstituted cyclopentenes.[34] Inspired by these recent achievements and aiming at identifying potential targets for experimental realization, we herein investigate the electronic structure, bonding situation, and stability of group 13, 14, and 15 main-group element homodimers coordinated to NDI. We are particularly interested in describing the proximity-enforced E···E interaction (Figure 1B), which is analyzed in detail using distinct computational approaches.

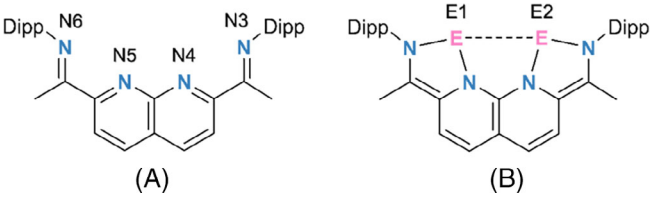

FIGURE 1 Structure of (A) naphthyridine diimine (NDI) and (B) a generalized NDI-E_2 complex (E = group 13–15 element).

2 | METHODS

Initially, we performed DFT geometry optimizations and frequency calculations at the M06[35]-D3[36]/def2-SVP[37] level of theory. This DFT functional was chosen since it provided the best structural agreement with the available experimental x-ray data according to our preliminary benchmark investigation. For all cases, we investigated the possibility of open-shell singlets by performing unrestricted DFT computations and selected multiconfigurational calculations at the CASSCF level.[38] The def2-ECP effective core potential was used for all elements heavier than Kr. All optimized structures were characterized as minimum energy geometries by vibrational frequency analyses. The bonding situation of the systems, particularly the proximity-enforced E···E interaction, was investigated using distinct approaches, namely the Mayer bond order (MBO),[39] quantum theory of atoms in molecules (QTAIM),[40] electron localization function (ELF),[41] intrinsic bond orbital (IBO),[42] and natural bond orbital (NBO)[43] techniques. Furthermore, the aromaticity of the compounds was investigated by means of the anisotropy of the current-induced density (ACID)[44] and nucleus-independent chemical shift (NICS)[45] methods, the latter using the def2-TZVP basis set. Finally, we also extended our analysis to the characterization of various stability parameters (vide infra). The geometry optimizations, vibrational frequencies and NICS calculations were done in Gaussian 16, revision C.01.[46] Multiconfigurational calculations were performed with Orca 5.0.3,[47] while the MBO, QTAIM, and ELF analyses were done with Multiwfn 3.8.[48] IBOs were obtained with the IBOview software.

3 | RESULTS AND DISCUSSION

3.1 | Analysis of structural and bonding properties

The geometry optimizations revealed that all NDI-E_2 systems (except E = P) possess only one low-lying equilibrium structure. Trends for the E1–N5–N4–E2 dihedral angles (see Figure 1 for the atom numbering) and the E–E bonding distance are given in Figure 2, which also contains the computed MBOs of the E–E bond. The computed equilibrium structures are depicted in Figures S1–S3 while Tables S1 and S2 contain the corresponding geometrical parameters. The QTAIM data is summarized in Table S3, while selected plots are depicted in Figure S4. Figure 3 depicts the ELF basins and attractors for selected compounds and Table S4 lists the corresponding values (ELF, N, σ^2, and λ). Finally, NBO and IBO analyses of the interaction between the main-group elements E are given in Figures 4 and 5 and Figure S5. The pyridine moiety of NDI shows aromaticity, which is strongly modified in the NDI complexes; Figure 6A and Figures S8–S10 consequently give the variations in the minimum of the $NICS_{zz}$ curves while Figure 6B and Figures S12–S14 give the π-ACID plots for the compounds.

The strong variations in the bonding situation of the NDI-E_2 complexes are already reflected in their geometries (Figure 2 and Figure S1–S3, Tables S1 and S2). Going from E = B to E = Tl, the E1–

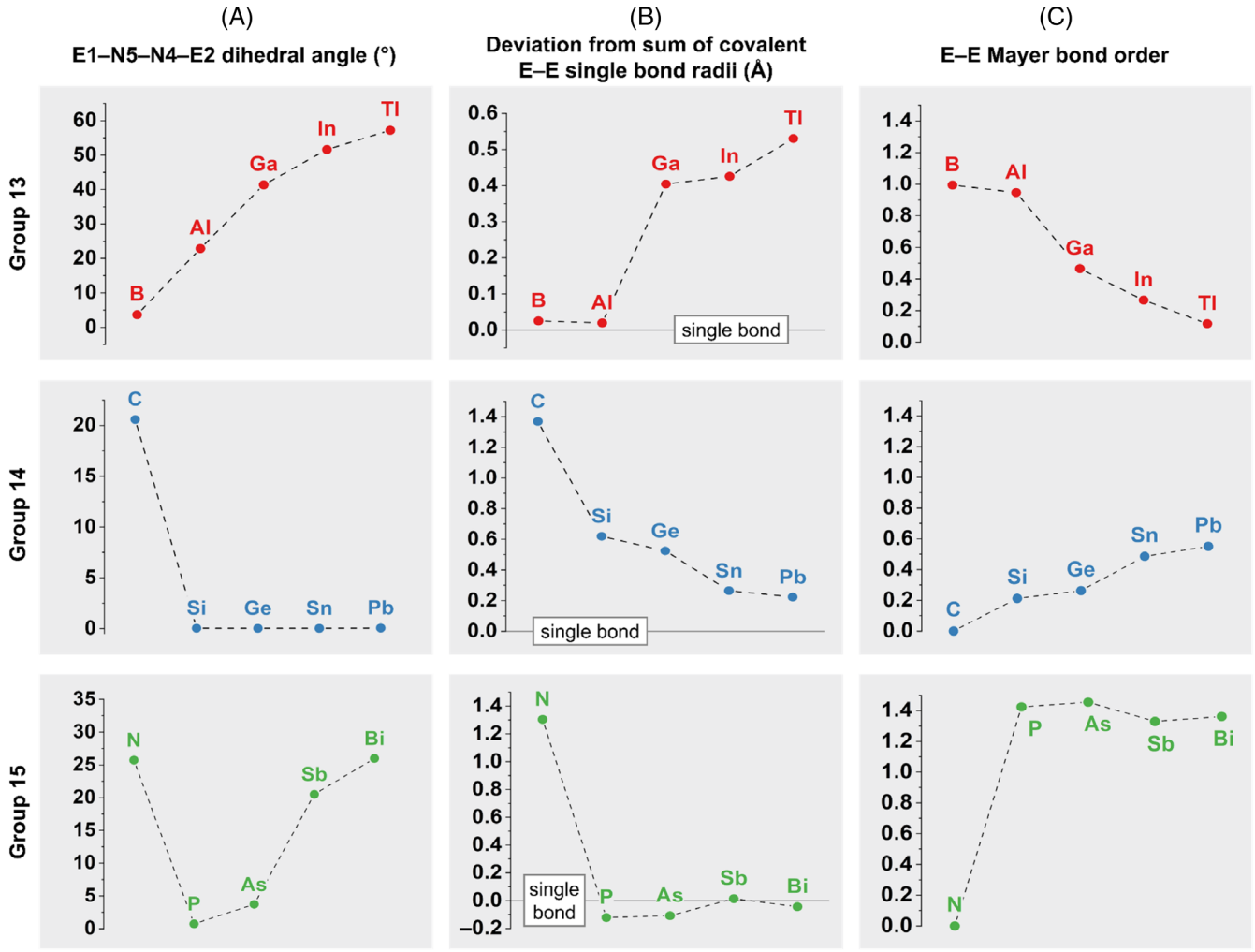

FIGURE 2 E1–N5–N4–E2 dihedral angle (A), deviation of E–E distance from sum of covalent single bond radii in Ångstrøm (B) and E–E Mayer bond order (C) of all compounds.

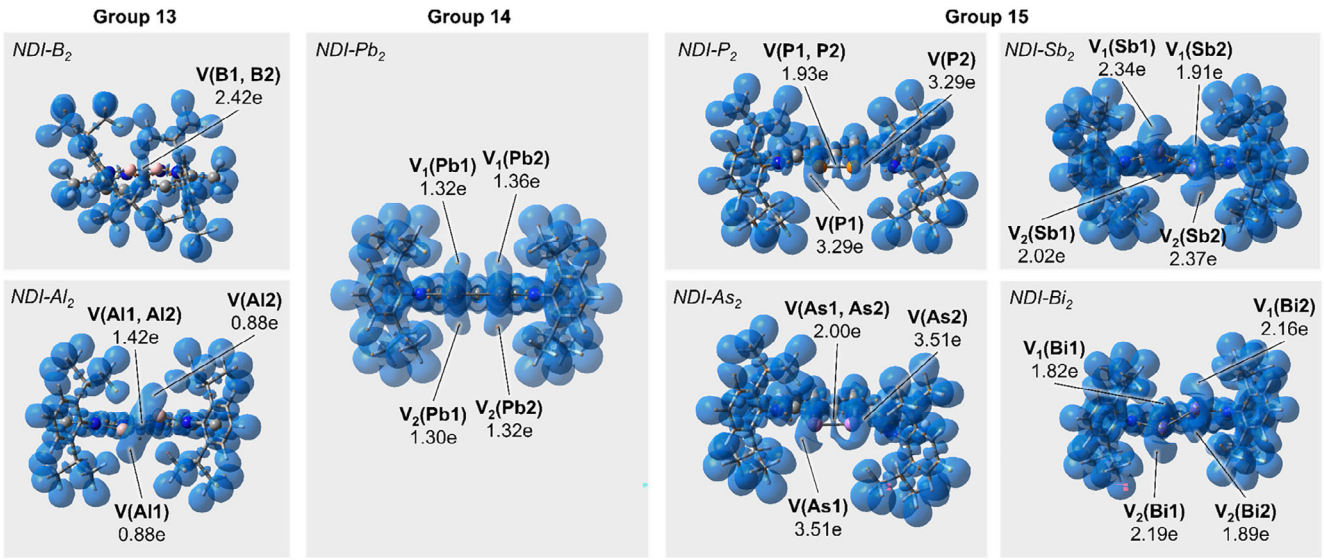

FIGURE 3 Electron localization function basins and attractors for E = B, Al, Pb, P, As, Sb, and Bi complexes with respective population numbers.

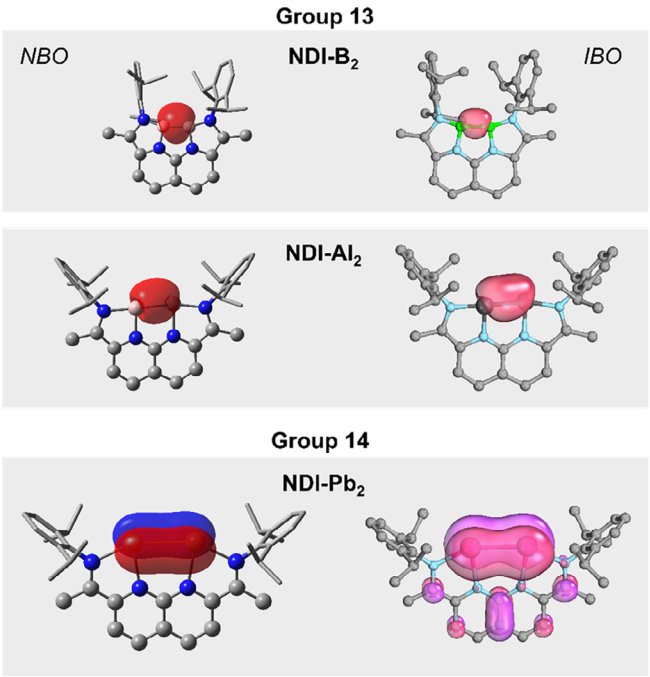

FIGURE 4 NBO (red and blue) and IBO (light red and pink) analysis of the bonding interaction between main-group element centers in E = B, Al and Pb complexes. IBO, intrinsic bond orbital; NBO, natural bond orbital.

N5–N4–E2 dihedral angle and the distance between both element centers each increase strongly. While E = B and E = Al are in the range of the sum of covalent single bond radii,[49] E = Ga–Tl exhibit much larger distances, though still ranging below the sum of the corresponding van der Waals radii (Table S1). This behavior is in line with the MBOs, which decrease from 0.99 for B and 0.95 for Al to 0.12 for Tl. This situation is reversed for the group 14 elements: For E = C, the dihedral angle is about 20° while planar geometries are found for E = Si–Pb. Additionally, the E–E distance approaches the sum of the covalent single bond radii with progression toward the heavier elements of group 14: the computed Si–Si distance is 2.94 Å which compares with 2.32 Å for the sum of covalent single bond radii. The corresponding values for E = Pb are 3.10 and 2.88 Å, respectively. Only for E = C is the E–E distance (2.87 Å) much larger than the sum of the covalent single bond radii. The geometrical variations again correlate with the MBOs, which increase from 0.21 (E = Si) to 0.55 (E = Pb). The E = N compound differs from the others in that it possesses a triplet ground state, while all other systems exhibit singlet ground states (see Figure 8 and Table S8). This was independently confirmed by a complementary state-specific CASSCF(2,2) calculation (SOMOs in Figure S15). For group 15 the data obtained for E = Sb and Bi resemble each other but notably differ from those computed for E = P and As. The differences become clear when looking at the corresponding equilibrium geometries depicted in Figure S3. For E = N the molecule is twisted and the E–E distance (2.72 Å) is considerably larger than the sum of the covalent single bond radii (1.42 Å), which can be rationalized by its triplet ground state. While non-planar structures are found for E = Sb and Bi, the E–E distances agree with the single bond distances. The differences are reflected in the Mayer bond order, which is negligible for E = N but is slightly larger than 1 for E = Sb and Bi. Hence, the deviations from planarity found for E = Sb and Bi result from the increasing steric demands of the main group element centers. For the E = P and As systems we predict nearly planar structures. The Mayer bond orders are 1.42 and 1.45, respectively, which is reflected in E–E bond distances that are slightly smaller than the sum of the covalent single bond radii, even approaching the sum of covalent double bond radii[50] (2.04 Å for P and 2.28 Å for As). These two compounds differ from all others because the element centers do not form bonds with N6 (R[P1–N6] = 2.57 Å, R[As1–N6] = 2.57 Å) or N3 (R[P2–N3] = 2.57 Å, R[As2–N3] = 2.57 Å) but instead create a five membered ring including E1, E2, N5, N4 and the adjacent carbon atom. For all other compounds, the distances of E to the adjacent nitrogen atoms N5, N4, N6, and N3 are in the range of single bonds. For E = P, the five-membered ring structure is 3.6 kcal mol^{-1} lower in energy than the expected form (bonding to N6 and N3) and both represent minima. For E = As, the structure with bonds to all adjacent nitrogen centers of the NDI moiety does not represent a minimum (see Figure S16 and Table S10).

The computed geometries reflect the strong variations in the bonding situation as a function of E. While various effects were expected, the computations reveal some unexpected outcomes, for example, the geometries of the E = P and As systems. To gain more insight into the bonding situation, we computed the electron densities ρ and their Laplacian ($\nabla^2\rho$) at the bond critical points (BCPs). These are summarized in Table S3 while selected plots (E = B, Ga, Si, P, Bi) are given in Figure S4. Table S3 shows that significant values relevant for (covalent) bonding are only met for E = B, P, and As. All other values are below 0.1, which does not allow for unambiguous interpretation. For E = B, P, and As, the computed values of ρ and $\nabla^2\rho$ indicate concentration of electron density rather than depletion, supporting the presence of classic covalent E–E bonds.

Complementary ELF analysis (see Table S4 for more details) also yields bonding basins between the main-group element centers for E = B, Al, P and As. In contrast, while E = Pb, Sb, and Bi possess large MBO values, the corresponding ELF valence basins are much more akin to lone pairs (Figure 3). Even though no formal bonding basins can be found for E = Pb and especially E = Sb and Bi, there is still a possibility of delocalized bonding interactions, which ELF fails to consider by its very nature of providing basins only related to the local pairing of electrons. Thus, further insight into the bonding situation of these compounds is necessary.

To further illuminate the bonding in the various compounds, in particular through the lens of localized, Lewis-like interaction, NBO and IBO analyses are good choices. Evaluation of the Lewis-like interactions between the main-group element centers yields bonding interaction for various compounds, pictured in Figures 4 and 5 (see Table S5 for corresponding values and Figure S5 and Table S6 for compounds not exhibiting binding E–E interaction).

Consistent with previous analyses, E = B and Al each show a σ-type single bond localized between the main-group element centers

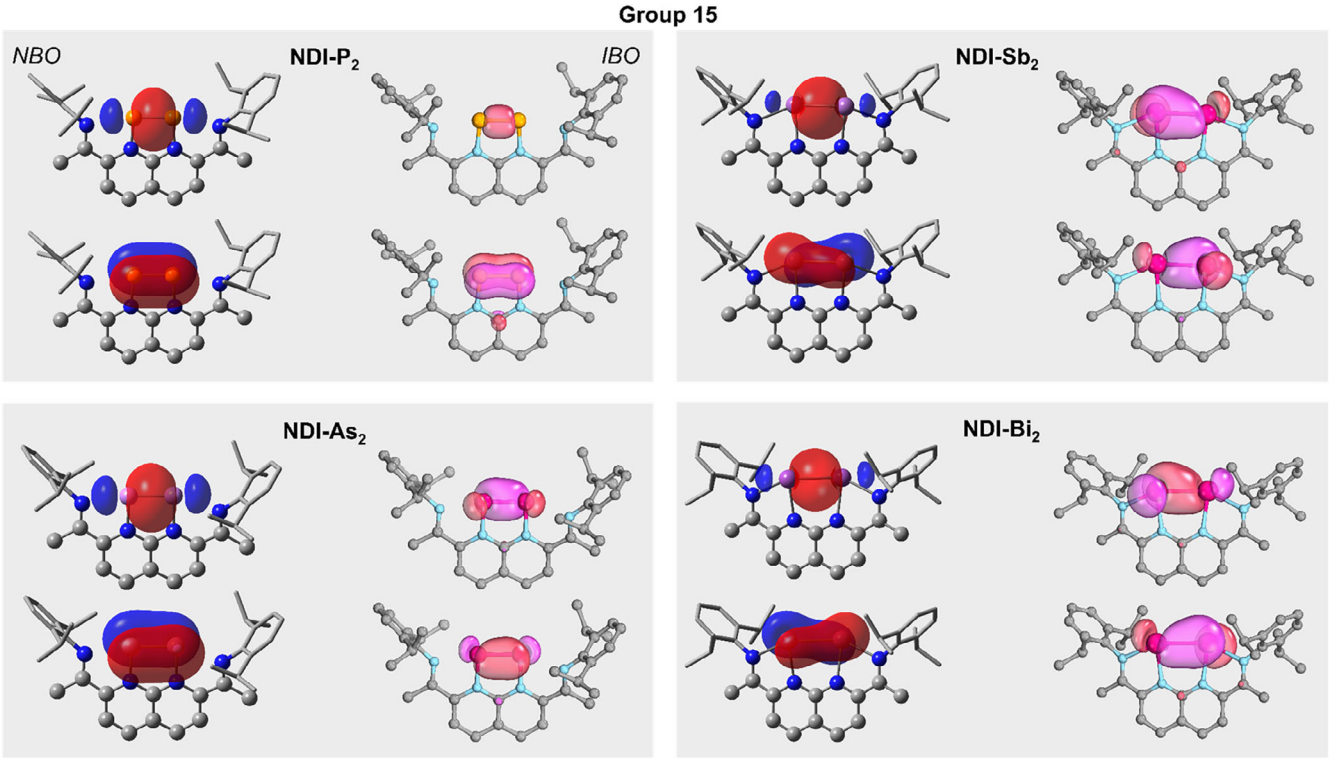

FIGURE 5 NBO (red and blue) and IBO (light red and pink) analysis of the bonding interaction between main-group element centers in E = P, As, Sb and Bi complexes. IBO, intrinsic bond orbital; NBO, natural bond orbital.

in both NBO and IBO analyses. For group 14 compounds, both methods point to non-interacting lone pairs at the element centers (Figure S5), which is in line with the corresponding ELF results. Only E = Pb shows an unusual through-space π-type bond[51] without an accompanying σ bond. The natural higher level of delocalization of this π bond explains the lack of bonding basins in the ELF analysis as well as the high electron fluctuation values of the respective valence basins (Table S4). NDI-E_2 systems where E = P and As exhibit a double bond structure in NBO analysis, consisting of a dedicated σ- and π-type bonding interaction. While this view is consistent with the NBOs and IBOs of the E = P system, the IBO analysis of E = As suggests a dative bond character with alternating donor–acceptor interactions between the two As center atoms. The same inconsistency can be observed for E = Sb and Bi, with IBO occupation numbers pushing even further in the direction of dative interaction (Table S5). Analysis of the adjacent N–E bonds further suggests a gradual shift from (polar) covalent bonding to dative bonding as well, correlating with the decreasing electronegativity of the element centers (Figure S6).

Looking at the broader geometrical structure of these compounds, it is also of interest how the formation of new ring structures influences the aromaticity of the whole system in comparison to the lone NDI ligand. Insights can be obtained by analyzing the minima of $NICS_{zz}$ scans as well as π ACID plots.

Figure 6 depicts the overall trends for the minima of the $NICS_{zz}$ curves together with the values obtained for the "naked" NDI (Figure 6A) and π ACID plots for E = P and As (Figure 6B). The corresponding data for all other compounds is given in Figures S8–S10, S12–14, and Table S7. For comparison, Figure S7 gives the $NICS_{zz}$ curves of the NDI while Figure S11 gives the π ACID plot of the NDI.

The NICS calculations revealed the newly formed five-membered rings to be highly aromatic, at the cost of losing aromaticity within the *napy* moiety relative to that of the unbound NDI ligand. For the sake of this discussion, the minimum values of the $NICS_{zz}$ curve for the marked orange and purple regions are sufficient for evaluation of overall aromaticity, a full breakdown of the NICS curves can be found in the SI (Figures S8–S10). Interestingly, even the nominally open pseudo-ring structures (see Figures S8–S10 for details) exhibit significant minima of the $NICS_{zz}$ curve, which are considered to be artifacts caused by the presence of strong neighboring aromatic rings.[52] The $NICS_{zz}$ values generally decline with progression toward heavier element centers, meaning a decrease of overall aromaticity, especially in group 13 and 15 compounds. $NICS_{zz}$ alone cannot distinguish between non-aromatic and antiaromatic behavior, however, this overall decline of aromaticity is also observed in complementary π ACID plots with the clockwise diatropic π electron ring current similarly fading alongside the progression toward heavier elements E, the *napy* moiety ultimately becoming non or even antiaromatic in case of E = Sb and Bi (see Figures S12–S14). Due to their unusual geometry, E = P and As also exhibit antiaromaticity alongside the *napy* moiety, this stands in contrast to the expected aromatic behavior of the anticipated geometries (Figure 6B).

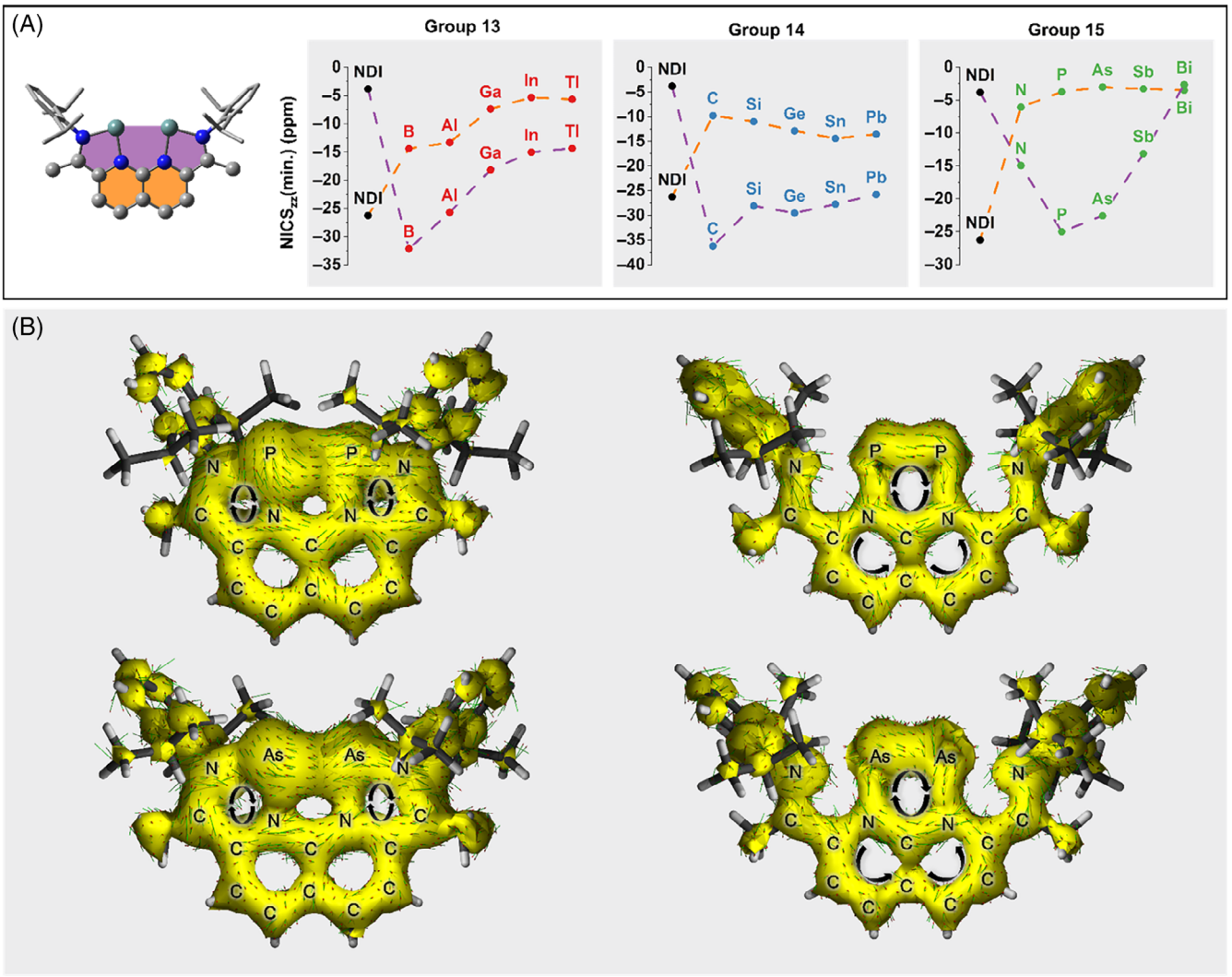

FIGURE 6 Minima of the NICS$_{zz}$ curve for the orange and purple regions for all compounds in comparison to the naked naphthyridine diimine ligand (A). π ACID plots of the phosphorus and arsenic systems with their bidentate analogs for comparison (B).

3.2 | Interpretation of bonding features

The Lewis structures depicted in Figure 7 give plausible bonding situations for the various NDI-E$_2$ systems. For group 13, E possesses three valence electrons, which could allow the formation of up to three covalent bonds. In principle, the E–E bond multiplicity could have any value between 0 and 3. For E = B, all bonding descriptors indicate the singly bound, left Lewis structure to be the major one. We predict a planar structure with an E–E distance equal to the sum of the covalent single bond radii and a Mayer bond order of ca. 1. Additionally, QTAIM analysis finds a concentration of density for the BCP of the B–B bond that is consistent with the ELF values. Finally, both NBO and IBO also predict a single σ bond. In contrast, for E = Ga, In and Tl, the descriptors indicate that the right Lewis structure, with no E–E bond, includes the most important binding effects. NBO and IBO clearly depict lone pairs (Figure S5), which is in line with negligible electron densities between both centers. Lone pairs are also indicated by the ELF values (Table S4), which find only one valence basin for each element center. Indeed, due to the decreasing ability to form multiple bonds and the expectedly lower E–E σ bond strength, the formation of lone pairs is preferred for these heavier elements. While the situation is quite clear for E = B, Ga, In, and Tl, it is somewhat more ambiguous for E = Al. Even though the E–E distance, Mayer bond order, NBOs and IBOs clearly indicate a bonding interaction similar to E = B, the QTAIM and ELF data are not that distinct. Nevertheless, based on the geometries, the NBO and the IBO data, we assume an E–E σ bond for E = Al.

Going to group 14 elements, each center possesses one additional electron. Consequently, for non-dative N–E bonds, carbene-like structures can be formed (Lewis structure on the left hand side). Assuming a dative N–E interaction, an additional single bond is possible. Based on the Mayer bond order and the E–E distance, mainly the former is found for E = C, Si, and Ge. For these systems, the E–E bond distance is considerably larger than the sum of the covalent single bond radii and the NBO/IBO analyses point to lone pairs located at the element centers. Such lone pairs are also indicated by the ELF. For

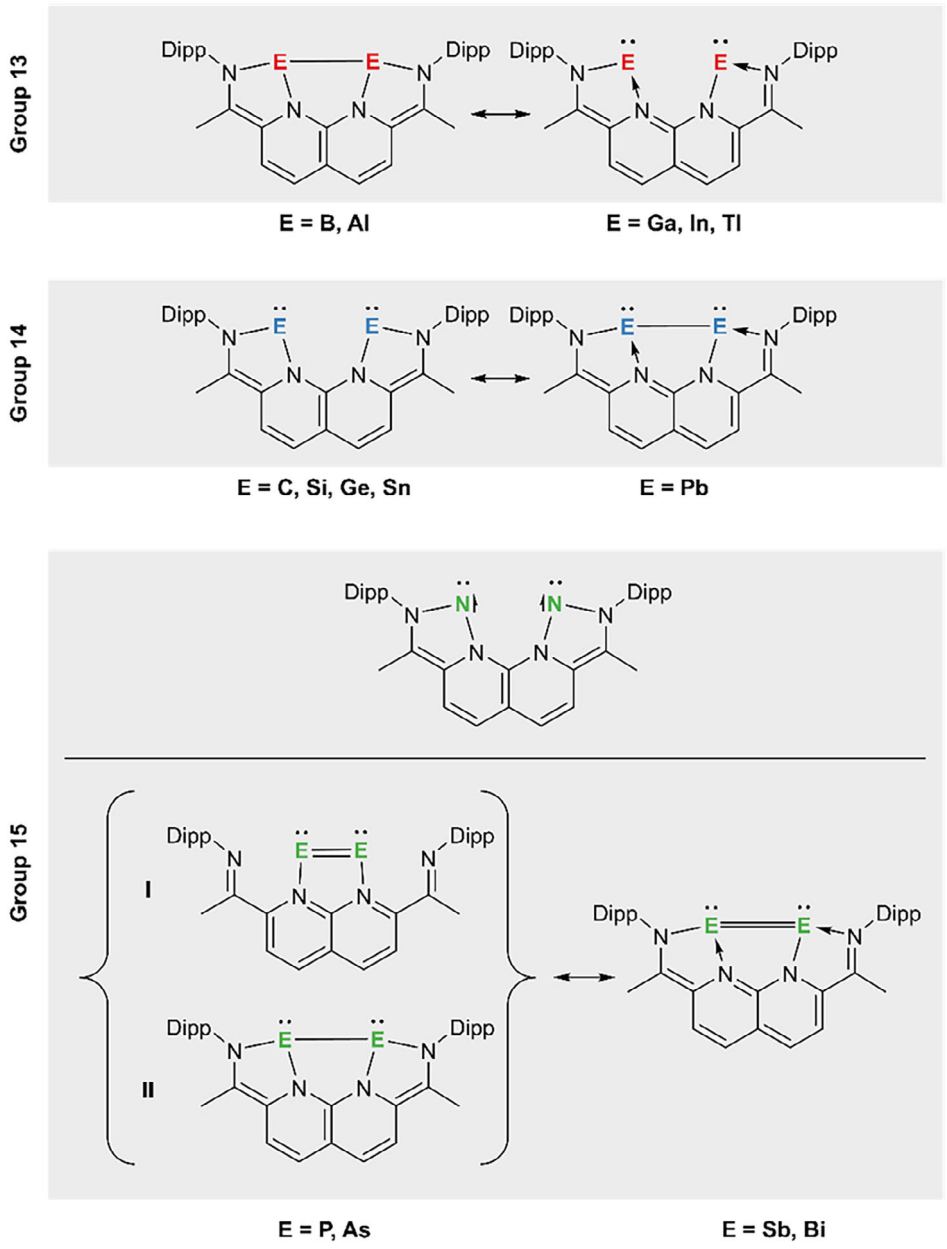

FIGURE 7 Possible Lewis structures for the calculated naphthyridine diimine compounds, separated by group.

E = Pb, the bonding situation reflects the right Lewis structure. Unexpectedly, the NBO/IBO results do not indicate the presence of a σ bond but instead a π bond. This picture is supported by the ELF data (Figure 3) which does not show bonding basins but high electron fluctuation values of the respective valence basins. While the bonding situations are quite clear for E = C, Si, Ge, and Pb, the Sn derivative lies somewhere between both Lewis structures. IBO and NBO analyses clearly indicate a similar situation found for the lighter elements; the Mayer bond order is closer to the value for E = Pb than to that of the lighter elements. The same holds true for the ELF data. For groups 13 and 14, the variations in bonding can be explained by two Lewis structures that naturally result from the number of valence electrons at the element centers assuming dative or non-dative N–E interaction, though the observed gradual shift in the N–E interaction cannot be properly expressed within the boundaries of the Lewis formalism. So far, only the through-space π bond found for E = Pb is unexpected, however it may result from suppressed hybridization typical for such heavy elements. It is also worth mentioning that no biradicaloid character was found for this system, excluding an open-shell singlet ground state. Looking at the computed geometries, the E–N bonds might be formed from non-hybridized in-plane p orbitals. The remaining out-of-plane p orbital would then form a formal π bond, which, due to the E–E distance, is quite weak. This is in line with a Mayer bond order of 0.55.

Except for E = Pb, the bonding situations found for groups 13 and 14 are expected, judging from the number of outer electrons and possible dative E–N bonds. In contrast, for group 15 compounds, our computations predict unexpected situations. Compound E = N possesses a triplet ground state, while closed-shell singlet ground states were predicted for all other systems. E = P and As also differ from all

other compounds in that the E–E bond is strengthened at the expense of the outer E–N bonds. The E = P isomer in which the E1–N6 (E2–N3) bond is broken but a E = E double bond is formed (isomer **I**), is computed to be 3.6 kcal mol^{-1} lower in energy than the corresponding bonded isomer in which E1 forms single bonds to N6 and N5 and E2 to N4 and N3 (isomer **II**). Nevertheless, **II** is still a minimum for E = P. In contrast, for E = As the corresponding isomer **II** is not a minimum energy structure. The NBO/IBO analyses indicate a regular σ/π double bond for isomer **I** (E = P, As) in contrast to E = Pb, for which only a π bond was found (vide supra). For E = Sb and Bi, the outcome of the NBO and IBO analyses differ. While the NBO analysis predicts σ/π bonding, IBO analysis clearly points to dative bonds. Although the unexpected ring formation in E = P and As compounds and the triplet ground state of E = N break the anticipated structural trend for group 15 compounds, they are not entirely unexplainable: Considering the atomic radii of the element centers, E = P and As occupy a unique window within group 15 compounds where both isomers can (and in the case of E = P will) be formed. Formation of an in-plane E = E double bond is accompanied by net negative energetics relative to formation of two N–E bonds and a possible out-of-plane E–E single bond. In comparison, Sb and Bi centers are too large for the rigid NDI cavity to not interact with N3 and N6 so only one isomer is possible. An E = E double bond can still be formed due to increased size of E and typical bonding distances. E = N, at the other end of the spectrum, is too small and typical N–N bonds are consequently too short to bridge the N–N gap without significant distortion of the NDI ligand (NDI distortion due to E–E bond formation can be observed in the E = B compound as an extreme case). E = N then defaults to a triplet ground state because of unpaired electrons at the element centers.

The size of the center atoms also defines the aromaticity: The five-membered rings increasingly break planarity of the system due to increasing size of E, much to the detriment of the overall aromaticity of the plane established by the *napy* moiety of the NDI. It is also worth noting that with progression toward heavier elements, the NDI nitrogen lone pairs become increasingly involved in dative E–N bonding as discussed above (Figure S6), relegating them toward the σ space where they cannot participate in the aromatic π system. This can also be observed in the ACID plots, where the ring current recedes along the N–E bond axes with progression toward the heavier element centers.

Although group 15 compounds yield a higher amount of unexpected structures, the generally observed trend of (gradual) change in E–N interaction going from lighter to heavier elements of each group still holds true. Correlating with the increasing electronegativity difference of E and N, this in turn changes the E–E interaction according to the availability of outer electrons at the element centers.

3.3 | Predictions for dimer stability

With the characterization of the geometry and bonding situation formally settled, we conducted a follow up investigation to gain more insight into the stability of the compounds. Evaluation of the HOMO-LUMO and singlet–triplet gaps proved to be a good starting point (Figure 8 and Table S8): The dimers consisting of main group elements from group 14 show the highest HOMO-LUMO and singlet–triplet gaps, narrowing from lighter to heavier elements (3.74 eV and 39.8 kcal mol^{-1} for E = C and 2.30 eV and 22.9 kcal mol^{-1} for Pb, respectively) while the dimers of groups 13 and 15 (with the exception of E = B) cluster around the lower end of the spectrum at ca. 2.25 eV and 10 kcal mol^{-1}. E = N exhibits the previously mentioned triplet ground state with a singlet–triplet gap of only −2.7 kcal mol^{-1} whereas E = B proves to be surprisingly stable in comparison to its heavier homologs with a HOMO-LUMO and singlet–triplet gap rivaling those of E = C (3.72 eV and 42.0 kcal mol^{-1}, respectively). E = P shows a singlet–triplet gap ca. 15 kcal mol^{-1} above the values observed for the majority of the group 15 dimers, placing itself in the vicinity of E = Si and Ge.

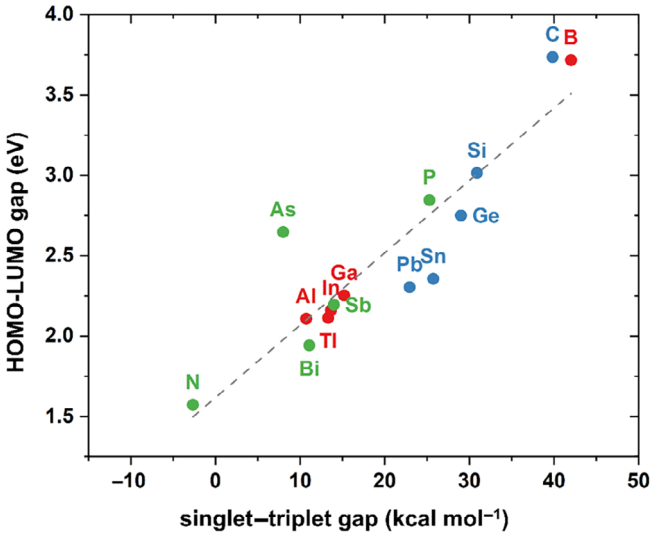

FIGURE 8 Singlet–triplet gaps in kcal mol^{-1} plotted against HOMO-LUMO gaps in eV. A linear fit was applied.

To arrive at a more holistic understanding of stability in these dimer compounds, one could additionally consider the dissociation energies of the E–N bonds as another stability indicator. The problem with this approach, however, lies with the extreme instability of some of the unsupported E_2 systems.[53] For these cases, dissociation energies would consequently explode and therefore be of little physical meaning and comparative value. Furthermore, since not all the E_2 systems possess singlet ground states,[54] the construction of a general isodesmic reaction scheme involving these species is also insubstantial. In order to circumvent these problems, we performed the stability analysis utilizing the following reaction:

$$LGe_2 + 2\,EH_3 \rightarrow LE_2 + Ge_2H_6 \quad (1)$$

To avoid EH_3-type radicals when involving group 14 compounds, Equation (1) was slightly altered for the corresponding dimers, giving

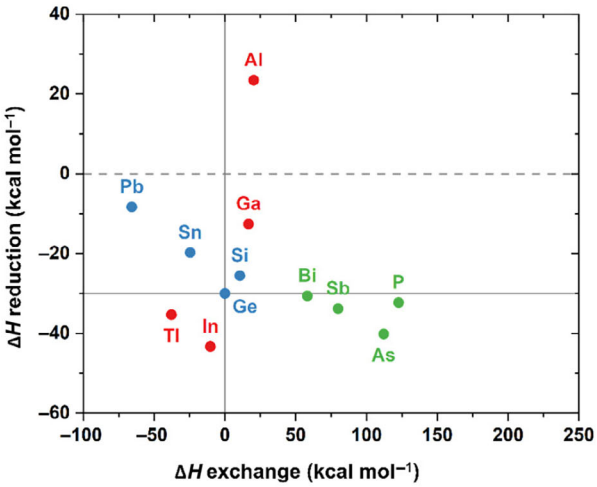

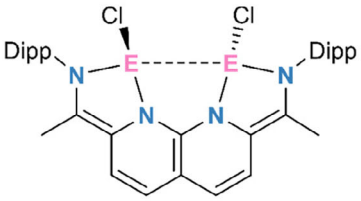

Reduction: $LE_2Cl_2 + \frac{1}{4}(Cp^*Al)_4 \rightarrow LE_2 + \frac{1}{2}(Cp^*AlCl_2)_2$

Exchange: $LGe_2 + 2\,EH_3 \rightarrow LE_2 + Ge_2H_6$ (Groups 13 and 15)

$LGe_2 + E_2H_6 \rightarrow LE_2 + Ge_2H_6$ (Group 14)

FIGURE 9 Reduction enthalpy of dichloro precursor plotted against exchange enthalpy as defined in the figure.

$$LGe_2 + 2\,E_2H_6 \rightarrow LE_2 + Ge_2H_6 \quad (2)$$

This scheme essentially quantifies the tendency of any main-group element E to favorably interact with the NDI ligand in direct comparison to the experimentally realized NDI-Ge_2 system.[33] A negative net enthalpy of the reaction for a given E would then indicate greater stability than that of the Ge system while a positive net enthalpy would suggest the opposite.

To add another dimension to our analysis, we also sought ways to incorporate aspects of the synthesis of the NDI-Ge_2 system[33] into a stability indicator. We consequently adapted the last reduction step of the experimental procedure to our systems and calculated the net enthalpy (referred to as ΔH reduction) of the reaction to use as a further stability indicator:

$$LE_2Cl_2 + \tfrac{1}{4}(Cp^*Al)_4 \rightarrow LE_2 + \tfrac{1}{2}(Cp^*AlCl_2)_2 \quad (3)$$

Although this may not be as simple an endeavor from the perspective of an experimentalist, this indicator is an attempt to better align our computational investigations with the actual experimental procedure.

The results are shown in Figure 9 and Table S9, with the net enthalpy of Equations (1) and (2) referred to as ΔH exchange (meaning hypothetical exchange of the Ge atoms in the bis(germylene) system with the respective elements E according to the reaction scheme). Due to the higher extent of orbital hybridization resulting in deviating properties in comparison to their heavier homologs, the compounds with E = B, C, and N have been omitted from the exchange axis to maintain close comparability to the Ge system. Furthermore, the dichloro precursor systems (pictured in Figure 9) for E = C and N unfortunately converged into dicationic structures with non-bound chloride counteranions, so their respective position on the reduction axis would be inaccurate.

The reduction of the dichloro precursor as described in Equation (3) is generally thermodynamically favored for all other compounds, with E = Al being the sole exception. A direct comparison with the reduction enthalpy of the bis(germylene) system shows that elements from groups 13 and 15 (E = In, Tl, P, As, Sb, Bi) generally possess more favorable ΔH reduction values, making them more stable than the NDI-Ge_2 system in respect to this stability indicator. Additional consideration of ΔH exchange (Equations 1 and 2) relative to that of the bis(germylene) system leaves only four compounds with overall lower net enthalpy, making the E = Sn, Pb, In and Tl systems interesting candidates for further experimental investigation. The E = Si and Ga systems also show some potential for synthesis since their net enthalpies of reduction and exchange still almost cancel out. Taking the HOMO-LUMO and singlet–triplet gaps into consideration, the homologs of the NDI-Ge_2 system (E = Si, Sn, and Pb) especially show overall comparable, if not higher stability than the bis(germylene). And while the E = B system shows exceptional stability through its HOMO-LUMO and singlet-triplet gaps, we anticipate that the strained geometry of NDI-B_2 as imposed by the B–B σ bond (Figure S1) might enforce additional challenges toward its experimental realization.

4 | CONCLUSIONS

In this work, we predicted the structures and bonding situations of 15 NDI-stabilized main-group dimers E_2 from groups 13, 14 and 15, utilizing various computational methods. Our analysis shows that a gradual change of the N–E and E–E interactions, correlating with decreasing electronegativity of the element centers, allow for different E–E bonding modes within each group of compounds. From the bonding situation perspective, notable compounds include the E = Pb system, where an unusual Pb–Pb π-only bond is observed, the E = N system which represents the only triplet ground state of our investigation, and the E = P and As systems. Due to the unique relation of their atomic radii and the size of the rigid NDI cavity, the systems where E = P and As have the ability to form an unexpected planar five-

membered ring including both element centers. This isomer is more stable than the formation of two five-membered rings containing one element center each, which is the preferred configuration of all other compounds. The analysis of aromaticity indices shows these newly formed five-membered C_2N_2E rings to be highly aromatic, though aromaticity fades upon progression to heavier elements due to increasing dative character of the interactions. The evaluation of distinct stability parameters predicts the NDI-E_2 systems wherein E = Ga, In, Tl, Si, Sn, and Pb to be potential targets for further experimental investigation.

ACKNOWLEDGMENT

H.B. gratefully acknowledges the Deutsche Forschungsgemeinschaft for funding. Open Access funding enabled and organized by Projekt DEAL.

DATA AVAILABILITY STATEMENT

The data that supports the findings of this study are available in the supplementary material of this article.

ORCID

Jonas Weiser https://orcid.org/0000-0001-6698-2519
Rian D. Dewhurst https://orcid.org/0000-0001-5978-811X
Holger Braunschweig https://orcid.org/0000-0001-9264-1726
Bernd Engels https://orcid.org/0000-0003-3057-389X
Felipe Fantuzzi https://orcid.org/0000-0002-8200-8262

REFERENCES

[1] (a) Y. Wang, G. H. Robinson, *Dalton Trans.* **2012**, *41*, 337. (b) H. Braunschweig, R. D. Dewhurst, *Angew. Chem. Int. Ed.* **2013**, *52*, 3574. (c) M. Arrowsmith, H. Braunschweig, T. E. Stennett, *Angew. Chem. Int. Ed.* **2017**, *56*, 96. (d) L. Zhao, S. Pan, N. Holzmann, P. Schwerdtfeger, G. Frenking, *Chem. Rev.* **2019**, *119*, 8781. (e) C. Poggel, G. Frenking, in *Advances in Inorganic Chemistry*, Vol. 73 (Eds: R. van Eldik, R. Puchta), Elsevier, Cambridge **2019**, p. 33. (f) P. P. Power, *Organometallics* **2020**, *39*, 4127.

[2] (a) P. P. Power, *Acc. Chem. Res.* **2011**, *44*, 627. (b) H. Braunschweig, T. Dellermann, R. D. Dewhurst, W. C. Ewing, K. Hammond, J. O. C. Jimenez-Halla, T. Kramer, I. Krummenacher, J. Mies, A. K. Phukan, A. Vargas, *Nat. Chem.* **2013**, *5*, 1025. (c) J. Böhnke, H. Braunschweig, T. Dellermann, W. C. Ewing, K. Hammond, J. O. C. Jimenez-Halla, T. Kramer, J. Mies, *Angew. Chem. Int. Ed.* **2015**, *54*, 13801. (d) M. Arrowsmith, J. Böhnke, H. Braunschweig, M. A. Celik, T. Dellermann, K. Hammond, *Chem. Eur. J.* **2016**, *22*, 17169. (e) M. Arrowsmith, J. Böhnke, H. Braunschweig, M. A. Celik, C. Claes, W. C. Ewing, I. Krummenacher, K. Lubitz, C. Schneider, *Angew. Chem. Int. Ed.* **2016**, *55*, 11271. (f) S. Yadav, S. Saha, S. S. Sen, *Chem Catal. Chem* **2016**, *8*, 486. (g) P. Bag, A. Porzelt, P. J. Altmann, S. Inoue, *J. Am. Chem. Soc.* **2017**, *139*, 14384. (h) A. Stoy, J. Böhnke, J. O. C. Jiménez-Halla, R. D. Dewhurst, T. Thiess, H. Braunschweig, *Angew. Chem. Int. Ed.* **2018**, *57*, 5947. (i) C. Weetman, A. Porzelt, P. Bag, F. Hanusch, S. Inoue, *Chem. Sci.* **2020**, *11*, 4817. (j) T. Brückner, F. Fantuzzi, T. E. Stennett, I. Krummenacher, R. D. Dewhurst, B. Engels, H. Braunschweig, *Angew. Chem. Int. Ed.* **2021**, *60*, 13661. (k) F. Schorr, F. Fantuzzi, R. D. Dewhurst, H. Braunschweig, *Chem. Commun.* **2021**, *57*, 2645. (l) K. Koshino, R. Kinjo, *J. Am. Chem. Soc.* **2021**, *143*, 18172. (m) L. Englert, U. Schmidt, M. Dömling, M. Passargus, T. E. Stennett, A. Hermann, M. Arrowsmith, M. Härterich, J. Müssig, A. Phillipps, D. Prieschl, A. Rempel, F. Rohm, K. Radacki, F. Schorr, T. Thiess, J. O. C. Jiménez-Halla, H. Braunschweig, *Chem. Sci.* **2021**, *12*, 9506. (n) W. Lu, A. Jayaraman, F. Fantuzzi, R. D. Dewhurst, M. Härterich, M. Dietz, S. Hagspiel, I. Krummenacher, K. Hammond, J. Cui, H. Braunschweig, *Angew. Chem. Int. Ed.* **2022**, *61*, e202113947. (o) F. Fantuzzi, Y. Jiao, R. D. Dewhurst, F. Weinhold, H. Braunschweig, B. Engels, *Chem. Sci.* **2022**, *13*, 5118.

[3] (a) T. Sugahara, J.-D. Guo, T. Sasamori, S. Nagase, N. Tokitoh, *Angew. Chem. Int. Ed.* **2018**, *57*, 3499. (b) C. Weetman, P. Bag, T. Szilvási, C. Jandl, S. Inoue, *Angew. Chem. Int. Ed.* **2019**, *58*, 10961. (c) J. Fan, J.-Q. Mah, M.-C. Yang, M.-D. Su, C.-W. So, *J. Am. Chem. Soc.* **2021**, *143*, 4993. (d) C. Weetman, *Chem. Eur. J.* **2021**, *27*, 1941. (e) P. Sreejyothi, K. Bhattacharyya, S. Kumar, P. K. Hota, A. Datta, S. K. Mandal, *Chem. Eur. J.* **2021**, *27*, 11656.

[4] (a) S. Würtemberger-Pietsch, U. Radius, T. B. Marder, *Dalton Trans.* **2016**, *45*, 5880. (b) V. Nesterov, D. Reiter, P. Bag, P. Frisch, R. Holzner, A. Porzelt, S. Inoue, *Chem. Rev.* **2018**, *118*, 9678.

[5] (a) M. Soleilhavoup, G. Bertrand, *Acc. Chem. Res.* **2015**, *48*, 256. (b) M. Melaimi, R. Jazzar, M. Soleilhavoup, G. Bertrand, *Angew. Chem. Int. Ed.* **2017**, *56*, 10046. (c) S. K. Kushvaha, A. Mishra, H. W. Roesky, K. C. Mondal, *Chem. Asian J.* **2022**, *17*, e202101301.

[6] (a) Y. Wang, B. Quillian, P. Wei, C. S. Wannere, Y. Xie, R. B. King, H. F. Schaefer, P. V. R. Schleyer, G. H. Robinson, *J. Am. Chem. Soc.* **2007**, *129*, 12412. (b) Y. Wang, B. Quillian, P. Wei, Y. Xie, C. S. Wannere, R. B. King, H. F. Schaefer, P. V. R. Schleyer, G. H. Robinson, *J. Am. Chem. Soc.* **2008**, *130*, 3298. (c) P. Bissinger, H. Braunschweig, M. A. Celik, C. Claes, R. D. Dewhurst, S. Endres, H. Kelch, T. Kramer, I. Krummenacher, C. Schneider, *Chem. Commun.* **2015**, *51*, 15917. (d) W. Lu, Y. Li, R. Ganguly, R. Kinjo, *J. Am. Chem. Soc.* **2017**, *139*, 5047. (e) W. Lu, Y. Li, R. Ganguly, R. Kinjo, *Angew. Chem. Int. Ed.* **2017**, *56*, 9829. (f) C. Pranckevicius, C. Herok, F. Fantuzzi, B. Engels, H. Braunschweig, *Angew. Chem. Int. Ed.* **2019**, *58*, 12893. (g) U. Schmidt, F. Fantuzzi, M. Arrowsmith, A. Hermann, D. Prieschl, A. Rempel, B. Engels, H. Braunschweig, *Chem. Commun.* **2020**, *56*, 14809.

[7] H. Braunschweig, R. D. Dewhurst, K. Hammond, J. Mies, K. Radacki, A. Vargas, *Science.* **2012**, *336*, 1420.

[8] J. Böhnke, H. Braunschweig, W. C. Ewing, C. Hörl, T. Kramer, I. Krummenacher, J. Mies, A. Vargas, *Angew. Chem. Int. Ed.* **2014**, *53*, 9082.

[9] C. Mohapatra, S. Kundu, A. N. Paesch, R. Herbst-Irmer, D. Stalke, D. M. Andrada, G. Frenking, H. W. Roesky, *J. Am. Chem. Soc.* **2016**, *138*, 10429.

[10] O. Back, G. Kuchenbeiser, B. Donnadieu, G. Bertrand, *Angew. Chem. Int. Ed.* **2009**, *48*, 5530.

[11] (a) J. D. Masuda, W. W. Schoeller, B. Donnadieu, G. Bertrand, *Angew. Chem. Int. Ed.* **2007**, *46*, 7052. (b) J. D. Masuda, W. W. Schoeller, B. Donnadieu, G. Bertrand, *J. Am. Chem. Soc.* **2007**, *129*, 14180.

[12] R. Kinjo, B. Donnadieu, G. Bertrand, *Angew. Chem. Int. Ed.* **2010**, *49*, 5930.

[13] (a) D. S. Weinberger, M. Melaimi, C. E. Moore, A. L. Rheingold, G. Frenking, P. Jerabek, G. Bertrand, *Angew. Chem. Int. Ed.* **2013**, *52*, 8964. (b) T. Hashimoto, R. Hoshino, T. Hatanaka, Y. Ohki, K. Tatsumi, *Organometallics* **2014**, *33*, 921. (c) K. C. Mondal, P. P. Samuel, H. W. Roesky, E. Carl, R. Herbst-Irmer, D. Stalke, B. Schwederski, W. Kaim, L. Ungur, L. F. Chibotaru, M. Hermann, G. Frenking, *J. Am. Chem. Soc.* **2014**, *136*, 1770.

[14] (a) K. C. Mondal, H. W. Roesky, M. C. Schwarzer, G. Frenking, B. Niepötter, H. Wolf, R. Herbst-Irmer, D. Stalke, *Angew. Chem. Int. Ed.* **2013**, *52*, 2963. (b) K. C. Mondal, S. Roy, H. W. Roesky, *Chem. Soc. Rev.* **2016**, *45*, 1080. (c) J. Böhnke, T. Dellermann, M. A. Celik, I. Krummenacher, R. D. Dewhurst, S. Demeshko, W. C. Ewing, K. Hammond, M. Heß, E. Bill, E. Welz, M. I. S. Röhr, R. Mitrić, B. Engels, F. Meyer, H. Braunschweig, *Nat. Commun.* **2018**, *9*, 1197. (d) D. Rottschäfer, B. Neumann, H.-G. Stammler, D. M. Andrada, R. S. Ghadwal, *Chem. Sci.* **2018**, *9*, 4970. (e) M. M. Hansmann, M. Melaimi, D. Munz, G. Bertrand, *J. Am. Chem. Soc.* **2018**, *140*, 2546. (f) D.

Rottschäfer, N. K. T. Ho, B. Neumann, H.-G. Stammler, M. van Gastel, D. M. Andrada, R. S. Ghadwal, *Angew. Chem. Int. Ed.* **2018**, *57*, 5838. (g) S. K. Mellerup, Y. Cui, F. Fantuzzi, P. Schmid, J. T. Goettel, G. Bélanger-Chabot, M. Arrowsmith, I. Krummenacher, Q. Ye, V. Engel, B. Engels, H. Braunschweig, *J. Am. Chem. Soc.* **2019**, *141*, 16954. (h) A. Deissenberger, E. Welz, R. Drescher, I. Krummenacher, R. D. Dewhurst, B. Engels, H. Braunschweig, *Angew. Chem. Int. Ed.* **2019**, *58*, 1842. (i) C. Saalfrank, F. Fantuzzi, T. Kupfer, B. Ritschel, K. Hammond, I. Krummenacher, R. Bertermann, R. Wirthensohn, M. Finze, P. Schmid, V. Engel, B. Engels, H. Braunschweig, *Angew. Chem. Int. Ed.* **2020**, *59*, 19338. (j) T. Ullrich, P. Pinter, J. Messelberger, P. Haines, R. Kaur, M. M. Hansmann, D. Munz, D. M. Guldi, *Angew. Chem. Int. Ed.* **2020**, *59*, 7906. (k) M. Rang, F. Fantuzzi, M. Arrowsmith, I. Krummenacher, E. Beck, R. Witte, A. Matler, A. Rempel, T. Bischof, K. Radacki, B. Engels, H. Braunschweig, *Angew. Chem. Int. Ed.* **2021**, *60*, 2963. (l) M. K. Sharma, F. Ebeler, T. Glodde, B. Neumann, H.-G. Stammler, R. S. Ghadwal, *J. Am. Chem. Soc.* **2021**, *143*, 121. (m) M. K. Sharma, D. Rottschäfer, T. Glodde, B. Neumann, H. Stammler, R. S. Ghadwal, *Angew. Chem. Int. Ed.* **2021**, *60*, 6414. (n) A. Maiti, F. Zhang, I. Krummenacher, M. Bhattacharyya, S. Mehta, M. Moos, C. Lambert, B. Engels, A. Mondal, H. Braunschweig, P. Ravat, A. Jana, *J. Am. Chem. Soc.* **2021**, *143*, 3687. (o) A. Maiti, B. J. Elvers, S. Bera, F. Lindl, I. Krummenacher, P. Ghosh, C. B. Yildiz, H. Braunschweig, C. Schulzke, A. Jana, *Chem. Eur. J.* **2022**, *28*, e202104567.

[15] (a) J. Messelberger, A. Grünwald, P. Pinter, M. M. Hansmann, D. Munz, *Chem. Sci.* **2018**, *9*, 6107. (b) E. Welz, J. Böhnke, R. D. Dewhurst, H. Braunschweig, B. Engels, *J. Am. Chem. Soc.* **2018**, *140*, 12580. (c) A. Japahuge, S. Lee, C. H. Choi, T. Zeng, *J. Chem. Phys.* **2019**, *150*, 234306. (d) P. Schmid, F. Fantuzzi, J. Klopf, N. B. Schröder, R. D. Dewhurst, H. Braunschweig, V. Engel, B. Engels, *Chem. Eur. J.* **2021**, *27*, 5160. (e) M. A. S. Francisco, F. Fantuzzi, T. M. Cardozo, P. M. Esteves, B. Engels, R. R. Oliveira, *Chem. Eur. J.* **2021**, *27*, 12126.

[16] M. Hermann, G. Frenking, *Chem. Eur. J.* **2017**, *23*, 3347.

[17] M. P. Mitoraj, A. Michalak, T. Ziegler, *J. Chem. Theory Comput.* **2009**, *5*, 962.

[18] R. Saha, S. Pan, P. K. Chattaraj, *ACS Omega* **2018**, *3*, 13720.

[19] (a) F. Fantuzzi, M. A. C. Nascimento, *Chem. Eur. J.* **2015**, *21*, 7814. (b) F. Fantuzzi, C. B. Coutinho, R. R. Oliveira, M. A. C. Nascimento, *Inorg. Chem.* **2018**, *57*, 3931.

[20] D. M. Andrada, G. Frenking, *Angew. Chem. Int. Ed.* **2015**, *54*, 12319.

[21] S. M. N. V. T. Gorantla, M. Francis, S. Roy, K. C. Mondal, *RSC Adv.* **2021**, *11*, 6586.

[22] M. Francis, S. Roy, *ACS Omega* **2022**, *7*, 5730.

[23] (a) A. Weiss, H. Pritzkow, P. J. Brothers, W. Siebert, *Angew. Chem. Int. Ed.* **2001**, *40*, 4182. (b) P. J. Brothers, *Advances in Organometallic Chemistry*, Vol. 48, Academic Press, Auckland **2001**, p. 289. (c) J. A. Cissell, T. P. Vaid, A. L. Rheingold, *J. Am. Chem. Soc.* **2005**, *127*, 12212. (d) J. A. Cissell, T. P. Vaid, G. P. A. Yap, *J. Am. Chem. Soc.* **2007**, *129*, 7841. (e) A. Weiss, M. C. Hodgson, P. D. W. Boyd, W. Siebert, P. J. Brothers, *Chem. Eur. J.* **2007**, *13*, 5982. (f) P. J. Brothers, *Chem. Commun.* **2008**, 2090. (g) T. P. Vaid, *J. Am. Chem. Soc.* **2011**, *133*, 15838. (h) Y. M. Sung, M. Vasiliu, D. A. Dixon, M. Bonizzoni, D. Kim, T. P. Vaid, *Photochem. Photobiol. Sci.* **2013**, *12*, 1774. (i) J. Conradie, P. J. Brothers, A. Ghosh, *Inorg. Chem.* **2019**, *58*, 4634. (j) J. E. Pia, B. A. Hussein, V. Skrypai, O. Sarycheva, M. J. Adler, *Coord. Chem. Rev.* **2021**, *449*, 214183.

[24] (a) T. Nyokong, *Coord. Chem. Rev.* **2007**, *251*, 1707. (b) T. Furuyama, K. Satoh, T. Kushiya, N. Kobayashi, *J. Am. Chem. Soc.* **2014**, *136*, 765.

[25] (a) I. Aviv-Harel, Z. Gross, *Coord. Chem. Rev.* **2011**, *255*, 717. (b) L. M. Reith, M. Koenig, C. Schwarzinger, W. Schoefberger, *Eur. J. Inorg. Chem.* **2012**, *2012*, 4342. (c) B. Basumatary, J. Rai, R. V. R. Reddy, J. Sankar, *Chem. Eur. J.* **2017**, *23*, 17458. (d) L.-G. Liu, Y.-M. Sun, Z.-Y. Liu, Y.-H. Liao, L. Zeng, Y. Ye, H.-Y. Liu, *Inorg. Chem.* **2021**, *60*, 2234.

[26] S. Biswas, N. Patel, R. Deb, M. Majumdar, *Chem. Rec.* **2022**, *22*, e202200003.

[27] (a) J. K. Bera, N. Sadhukhan, M. Majumdar, *Eur. J. Inorg. Chem.* **2009**, *2009*, 4023. (b) X. Gan, S.-M. Chi, W.-H. Mu, J.-C. Yao, L. Quan, C. Li, Z.-Y. Bian, Y. Chen, W.-F. Fu, *Dalton Trans.* **2011**, *40*, 7365. (c) B. Tsai, Y. Liu, S. Peng, S. Liu, *Eur. J. Inorg. Chem.* **2016**, *2016*, 2783. (d) A. Giordana, E. Priola, E. Bonometti, P. Benzi, L. Operti, E. Diana, *Polyhedron* **2017**, *138*, 239. (e) A. N. Desnoyer, A. Nicolay, P. Rios, M. S. Ziegler, T. D. Tilley, *Acc. Chem. Res.* **2020**, *53*, 1944. (f) E. Kounalis, M. Lutz, D. L. J. Broere, *Organometallics* **2020**, *39*, 585. (g) M. Piesch, A. Nicolay, M. Haimerl, M. Seidl, G. Balazs, T. D. Tilley, M. Scheer, *Chem. Eur. J.* **2022**, *28*, e202201144.

[28] (a) H.-J. Li, W.-F. Fu, L. Li, X. Gan, W.-H. Mu, W.-Q. Chen, X.-M. Duan, H.-B. Song, *Org. Lett.* **2010**, *12*, 2924. (b) Y.-Y. Wu, Y. Chen, G.-Z. Gou, W.-H. Mu, X.-J. Lv, M.-L. Du, W.-F. Fu, *Org. Lett.* **2012**, *14*, 5226. (c) M.-L. Du, C.-Y. Hu, L.-F. Wang, C. Li, Y.-Y. Han, X. Gan, Y. Chen, W.-H. Mu, M. L. Huang, W.-F. Fu, *Dalton Trans.* **2014**, *43*, 13924.

[29] J. Dipold, E. E. Romero, J. Donnelly, T. P. Calheiro, H. G. Bonacorso, B. A. Iglesias, J. P. Siqueira, F. E. Hernandez, L. De Boni, C. R. Mendonca, *Phys. Chem. Chem. Phys.* **2019**, *21*, 6662.

[30] L. Quan, Y. Chen, X.-J. Lv, W.-F. Fu, *Chem. Eur. J.* **2012**, *18*, 14599.

[31] (a) X. Liu, M. Chen, Z. Liu, M. Yu, L. Wei, Z. Li, *Tetrahedron* **2014**, *70*, 658. (b) G. F. Wu, Q. L. Xu, L. E. Guo, T. N. Zang, R. Tan, S. T. Tao, J. F. Ji, R. T. Hao, J. F. Zhang, Y. Zhou, *Tetrahedron Lett.* **2015**, *56*, 5034.

[32] J. Cui, M. Dietz, M. Härterich, F. Fantuzzi, W. Lu, R. D. Dewhurst, H. Braunschweig, *Chem. Eur. J.* **2021**, *27*, 15751.

[33] J. Cui, J. Weiser, F. Fantuzzi, M. Dietz, Y. Yatsenko, A. Häfner, S. Nees, I. Krummenacher, M. Zhang, K. Hammond, P. Roth, W. Lu, R. D. Dewhurst, B. Engels, H. Braunschweig submitted for publication

[34] Y.-Y. Zhou, D. R. Hartline, T. J. Steiman, P. E. Fanwick, C. Uyeda, *Inorg. Chem.* **2014**, *53*, 11770.

[35] Y. Zhao, D. G. Truhlar, *Theor. Chem. Acc.* **2008**, *120*, 215.

[36] S. Grimme, J. Antony, S. Ehrlich, H. Krieg, *J. Chem. Phys.* **2010**, *132*, 154104.

[37] F. Weigend, R. Ahlrichs, *Phys. Chem. Chem. Phys.* **2005**, *7*, 3297.

[38] B. O. Roos, in *Adv. Chem. Phys. Ab Initio Methods Quantum Chem. Part 2*, Vol. *69* (Ed: K. P. Lawley), John Wiley & Sons, Chichester **1987**, p. 399.

[39] (a) I. Mayer, *Chem. Phys. Lett.* **1983**, *97*, 270. (b) I. Mayer, *Int. J. Quantum Chem.* **1984**, *26*, 151.

[40] (a) R. F. W. Bader, *Chem. Rev.* **1991**, *91*, 893. (b) R. F. W. Bader, *J. Phys. Chem. A* **1998**, *102*, 7314.

[41] (a) A. D. Becke, K. E. Edgecombe, *J. Chem. Phys.* **1990**, *92*, 5397. (b) B. Silvi, A. Savin, *Nature* **1994**, *371*, 683. (c) A. Savin, B. Silvi, F. Colonna, *Can. J. Chem.* **1996**, *74*, 1088.

[42] G. Knizia, *J. Chem. Theory Comput.* **2013**, *9*, 4834.

[43] F. Weinhold, C. R. Landis, E. D. Glendening, *Int. Rev. Phys. Chem.* **2016**, *35*, 399.

[44] (a) R. Herges, D. Geuenich, *J. Phys. Chem. A* **2001**, *105*, 3214. (b) D. Geuenich, K. Hess, F. Köhler, R. Herges, *Chem. Rev.* **2005**, *105*, 3758.

[45] (a) Z. Chen, C. S. Wannere, C. Corminboeuf, R. Puchta, P. R. von Schleyer, *Chem. Rev.* **2005**, *105*, 3842. (b) J. O. C. Jiménez-Halla, E. Matito, J. Robles, M. Solà, *J. Organomet. Chem.* **2006**, *691*, 4359. (c) A. Stanger, *J. Org. Chem.* **2006**, *71*, 883. (d) A. C. Tsipis, *Phys. Chem. Chem. Phys.* **2009**, *11*, 8244.

[46] M. J. Frisch, G. W. Trucks, H. B. Schlegel, G. E. Scuseria, M. A. Robb, J. R. Cheeseman, G. Scalmani, V. Barone, B. Mennucci, G. A. Petersson, H. Nakatsuji, M. Caricato, X. Li, H. P. Hratchian, A. F. Izmaylov, J. Bloino, G. Zheng, J. L. Sonnenberg, M. Hada, M. Ehara, K. Toyota, R. Fukuda, J. Hasegawa, M. Ishida, T. Nakajima, Y. Honda, O. Kitao, H. Nakai, T. Vreven, J. A. Montgomery Jr., J. E. Peralta, F.

Ogliaro, M. Bearpark, J. J. Heyd, E. Brothers, K. N. Kudin, V. N. Staroverov, R. Kobayashi, J. Normand, K. Raghavachari, A. Rendell, J. C. Burant, S. S. Iyengar, J. Tomasi, M. Cossi, N. Rega, J. M. Millam, M. Klene, J. E. Knox, J. B. Cross, V. Bakken, C. Adamo, J. Jaramillo, R. Gomperts, R. E. Stratmann, O. Yazyev, A. J. Austin, R. Cammi, C. Pomelli, J. W. Ochterski, R. L. Martin, K. Morokuma, V. G. Zakrzewski, G. A. Voth, P. Salvador, J. J. Dannenberg, S. Dapprich, A. D. Daniels, Ö. Farkas, J. B. Foresman, J. V. Ortiz, J. Cioslowski, D. J. Fox, *Gaussian 16*, *Revision C.01*, Gaussian, Wallingford, CT **2016**.

[47] F. Neese, *Wiley Interdiscip. Rev. Comput. Mol. Sci.* **2012**, *2*, 73.

[48] T. Lu, F. Chen, *J. Comput. Chem.* **2012**, *33*, 580.

[49] P. Pyykkö, M. Atsumi, *Chem. Eur. J.* **2009**, *15*, 186.

[50] P. Pyykkö, M. Atsumi, *Chem. Eur. J.* **2009**, *15*, 12770.

[51] M.-J. Cheng, C.-H. Hu, *Mol. Phys.* **2003**, *101*, 1319.

[52] M. Solà, F. Feixas, J. O. C. Jiménez-Halla, E. Matito, J. Poater, *Symmetry* **2010**, *2*, 1156.

[53] W. M. Haynes Ed., *CRC Handbook of Chemistry and Physics*, 95th ed., CRC Press, Boca Raton, FL **2014**.

[54] B. O. Roos, R. Lindh, P.-Å. Malmqvist, V. Veryazov, P.-O. Widmark, *J. Phys. Chem. A* **2004**, *108*, 2851.

SUPPORTING INFORMATION

Additional supporting information can be found online in the Supporting Information section at the end of this article.

How to cite this article: J. Weiser, J. Cui, R. D. Dewhurst, H. Braunschweig, B. Engels, F. Fantuzzi, *J. Comput. Chem.* **2023**, *44*(3), 456. https://doi.org/10.1002/jcc.26994